



Theses and Dissertations

2019-07-01

DNA Capture via Magnetic Beads in a Microfluidic Platform for Rapid Detection of Antibiotic Resistance Genes

David Hyrum Harris
Brigham Young University

Follow this and additional works at: <https://scholarsarchive.byu.edu/etd>



Part of the [Biochemistry Commons](#), and the [Physical Sciences and Mathematics Commons](#)

BYU ScholarsArchive Citation

Harris, David Hyrum, "DNA Capture via Magnetic Beads in a Microfluidic Platform for Rapid Detection of Antibiotic Resistance Genes" (2019). *Theses and Dissertations*. 8633.

<https://scholarsarchive.byu.edu/etd/8633>

This Thesis is brought to you for free and open access by BYU ScholarsArchive. It has been accepted for inclusion in Theses and Dissertations by an authorized administrator of BYU ScholarsArchive. For more information, please contact ellen_amatangelo@byu.edu.

DNA Capture via Magnetic Beads in a Microfluidic Platform
for Rapid Detection of Antibiotic Resistance Genes

David Hyrum Harris

A thesis submitted to the faculty of
Brigham Young University
in partial fulfillment of the requirements for the degree of
Master of Science

Adam Woolley, Chair
Jaron Hansen
Aaron Hawkins

Department of Chemistry and Biochemistry
Brigham Young University

Copyright © 2019 David Hyrum Harris

All Rights Reserved

ABSTRACT

DNA Capture via Magnetic Beads in a Microfluidic Platform for Rapid Detection of Antibiotic Resistance Genes

David Hyrum Harris
Department of Chemistry and Biochemistry, BYU
Master of Science

Antibiotic resistant infections are a growing health care concern, with many cases reported annually. Infections can cause irreversible bodily damage or death if they are not diagnosed in a timely matter. To rapidly diagnose antibiotic resistance in infections, it is important to be able to capture and isolate the DNA coding for the resistance genes. This is challenging because bacteria are present in blood in minute concentrations. To enrich the DNA to detectable levels, I modified magnetic microbeads with ssDNA sequences complementary to the target DNA to capture the DNA via hybridization. I compared DNA capture efficiency in three different methods: Co-flow, packed bead bed, and pre-hybridization. The pre-hybridized method worked better than the other two. Since pre-hybridization involved mixing, I chose to study mixing in a microfluidic device. The mixing chamber was a well carved out of PMMA placed between two electromagnets. To test the mixing well, beads and capture DNA were placed in it, and the electromagnets were subjected to different frequencies, including symmetric or asymmetric magnetic fields. For each condition the capture efficiency was determined by measuring the relative fluorescence units (RFU). A 100 Hz asymmetric magnetic field had the best capture efficiency out of all conditions. These results demonstrate a path for enriching low concentrations of DNA to detectable levels, and future work should be done to develop electromagnetic mixing in microfluidic devices.

Keywords: microfluidics, magnetic microbeads, antibiotic resistance, sepsis

ACKNOWLEDGMENTS

I would like to thank my parents for pushing me to achieve the highest level of education. I looked to both of you with your Master's degrees as motivation for going to graduate school. Thank you for encouraging me to be patient and persistent even when things seemed difficult. Thank you for allowing me to talk to you when things were stressful or my plans were put abruptly to halt by forces I could not control.

I would also like to thank my advisor, Dr. Adam Woolley, for letting me work in his lab. I only had an engineering degree with minimal chemistry background, but he was still willing to take a risk with me. I also appreciate his guidance down the difficult path towards completing this thesis. I am also grateful for my committee members, both past and present for your encouragement. I appreciate the time that Drs. Jaron Hansen and Aaron Hawkins took to be on my committee, especially since a change was made on short notice.

I would also like to thank Drs. Bill Pitt and Daniel Austin, for being available when I had questions. Dr. Austin has a vast knowledge in magnetism and current which were important in this thesis. Dr. Pitt was always available when I had questions about fluids and mixing. I also appreciate Andy Monk, a graduate student in the Electrical and Computer Engineering Department for designing and fabricating the circuits I used for the electromagnetic micromixer.

I would like to thank the Department of Chemistry and Biochemistry at BYU for their facilities and resources, and the National Institutes of Health R01 AI116989 for funding. I am also grateful for a handful of undergraduate students I taught in recitation and labs. It was very satisfying hearing students say that I got them excited about chemistry.

TABLE OF CONTENTS

DNA Capture via Magnetic Beads in a Microfluidic Platform.....	ii
for Rapid Detection of Antibiotic Resistance Genes	ii
ABSTRACT.....	ii
ACKNOWLEDGMENTS	iii
TABLE OF CONTENTS.....	iv
LIST OF FIGURES	v
LIST OF TABLES.....	viii
1. INTRODUCTION.....	1
1.1- Sepsis.....	1
1.2- Current Methods for Diagnosing Antibiotic Resistance	1
1.3- Magnetic Microbeads for DNA Capture	3
1.4- Microfluidics	5
1.5- Microfluidic DNA Capture with Magnetic Microbeads in Sepsis Diagnosis	5
1.6- Summary of Thesis Work	9
2. DNA CAPTURE, ENRICHMENT AND DETECTION USING MAGNETIC MICROBEADS IN MICROFLUIDIC CHANNELS.....	10
2.1- Introduction	10
2.2- Experimental.....	10
2.3- Results.....	15
2.4- Discussion	21
2.5- Conclusion	22
3. FABRICATION OF ELECTROMAGNETIC MIXING CHAMBERS USING PRESSURE SENSITIVE ADHESIVES	23
3.1- Introduction	23
3.2- Experimental.....	23
3.3- Results.....	29
3.4- Conclusions.....	33
4. SUMMARY AND FUTURE WORK	35
4.1- Summary	35
4.2-Future Work	35
APPENDIX A-ARDUINO BASED AGITATION SYSTEM AND CODE.....	38
A.1- Wiring Diagram of EM Mixer	38
A.2- Code for Asymmetric Electromagnetic Mixer	39
A.3- Code for Symmetric Electromagnetic Mixer	40
BIBLIOGRAPHY	41

LIST OF FIGURES

Figure 1- Standard process for denaturing, capturing and labeling DNA. (a) Double stranded DNA is denatured by heating to 90 °C. (b) Target DNA hybridizes with ssDNA attached to the beads. (c) Beads with hybridized DNA will be pulled down by a magnet as all other DNA is rinsed through. (d) DNA hybridization probe with fluorescein attached will hybridize with the target DNA on the beads. (e) After heating DNA will de-hybridize and flow past a (f) focused 488 nm laser, inducing fluorescence and allowing the DNA to be detected. 4

Figure 2- The process of isolating, enriching, and detecting minute concentrations of DNA extracted from human blood. a.- Bacteria are separated from blood, lysed and then their DNA is extracted [43]. b.- Magnetic microbeads are used to enrich the target DNA to detectable levels c.- Optofluidics, with single molecule sensitivity, will be used to detect multiple gene sequences [45-47]. 6

Figure 3- Schematic for microfluidic chip for DNA capture. Double stranded DNA is introduced in the sample inlet and denatured in the serpentine channel, and the resulting ssDNA fragments are captured on the monolith. After heating, the DNA flows past a laser detector [49]. 8

Figure 4- A typical polypropylene chip with a Y channel. 11

Figure 5- Schematic depicting the experimental setup for a DNA capture and elution experiment. The inflow includes DNA and microbeads. The beads are trapped by the permanent magnet and all other material washes through. After heating, the released DNA is detected by fluorescence from the 488 nm laser excitation. 12

Figure 6- Standard process for capturing and enriching pre-labeled DNA. (a) Target DNA flows past magnetic beads, modified with a ssDNA complementary to the sequence of interest. (b) ssDNA complementary to the DNA on the bead will hybridize, and all other DNA will not. (c)

Magnetic beads with captured DNA will be pulled down by a magnet as all other DNA is rinsed through. (d) After heating, DNA will de-hybridize and flow through the channel. (e) The DNA will flow past a focused 488 nm laser, inducing fluorescence and allowing the DNA to be detected. 13

Figure 7- Calibration curve for an on-chip experiment using three different DNA concentrations. 15

Figure 8 – Fluorescent signal as a function of time during loading, capture and elution of 1 nM fluorescently labeled DNA. For this experiment beads and DNA flowed in the channel simultaneously. 16

Figure 9- Fluorescent signal as a function of time during loading, capture and elution of 1 nM fluorescently labeled DNA. Beads formed a packed bed before DNA flowed through the channel. 17

Figure 10- Fluorescent signal as a function of time during an experiment where 1 nM of fluorescently labeled target DNA was pre-hybridized with the capture sequence on the beads before being introduced in the channel. 18

Figure 11- Fluorescent signal as a function of time during an experiment where 1 nM of unlabeled dsDNA was de-hybridized, then captured and labeled on beads localized in a channel, and eluted. 19

Figure 12-SEM image of magnetic microbeads aggregated in a channel (left), and a zoomed in image of the boxed area (right). This image shows, that instead of filling the entire channel, the beads aggregated in brick-like structures. 21

Figure 13- A channel cut out of white 9965 double-sided adhesive that was placed directly above an imprinted channel with a 9969 layer. Different films were layered on top of 9965 for auto-fluorescence experiments..... 24

Figure 14- Wells used for electromagnetic mixing chambers a.- A circular well in PMMA, b.- A diamond shaped well..... 25

Figure 15- Two electromagnets connected in series with a mixing in between a.- Top view of a well with electromagnets placed directly above and beneath. b.- Side view of a well with electromagnets connected in series with a signal generator. 26

Figure 16- Capture electromagnets connected in series with an AC generator. a.- Schematic of the well, AC magnets and generator. b.- Photograph of the two AC magnets on each side of the mixing well. 27

Figure 17- General arrangement for Arduino based mixing experiments. The electromagnets were placed on either side of the mixing well, and were turned on in a pattern controlled by the chip..... 29

Figure 18- Δ RFU values for bead capture experiments in a circular well with flat cylindrical electromagnets. 31

Figure 19- Results for signal generator experiments using the diamond well..... 32

Figure 20- Results of the experiment using the Arduino Uno chip. 33

Figure 21- Design for a device with intersecting channels..... 36

Figure 22- Device with porous monolith. Beads aggregate behind the monolith. 36

LIST OF TABLES

Table 1- DNA capture and target sequence for the KPC antibiotic resistance gene.	11
Table 2- The average peak heights and estimated concentrations for each method. 1 nM was the loaded concentration for all experiments.	20
Table 3- 3M polymers that were evaluated.....	24
Table 4- The results of auto-fluorescence experiments for each polymer.....	30

1. INTRODUCTION

1.1- Sepsis

Sepsis is defined as organ dysfunction resulting from a host's response to an infection ^[1]. Such conditions are responsible for ~50% of all hospital deaths ^[2]. These infections are commonly from bacterial species in genera *Enterobacter* and *Klebsiella*, which can manifest symptoms with concentrations as low as 10 CFU/mL ^[3-5]. These infections are treated with antibiotics, antimicrobial agents active against bacteria ^[6]. However, point of care diagnosis of sepsis still needs to be improved to prevent the use of the wrong antibiotic, or unnecessary use of antibiotics, which has led to antibiotic resistance ^[7].

Antibiotic resistance is a growing healthcare concern with new cases being reported annually in multiple outbreaks, some of which show resistance to more than one antibiotic ^[8-10]. A survey of beta lactam resistance was conducted in multiple locations throughout the island of Puerto Rico, and antibiotic resistance genes were identified in isolates of at least 4 different bacterial species ^[9]. A similar survey in Brooklyn reported at least 10 different isolates from different hospitals around New York that were resistant to multiple antibiotics ^[10]. These studies demonstrate how widespread the issue of antibiotic resistance is.

Antibiotic resistant infections have a mortality rate as high as 50% with an increase of 7.9% every hour, and the possibility of irreversible brain damage in less than two hours ^[11, 12]. Thus, rapid new methods to diagnose antibiotic resistance are vital for patient survivability.

1.2- Current Methods for Diagnosing Antibiotic Resistance

An example of a current method is the diagnosis of vancomycin resistant *Staphylococcus aureus* (VISA). To determine if an infection is VISA, bacteria are cultured on plates with

varying vancomycin concentrations. The culture and incubation times for this method are approximately 48 hours ^[13]. Other methods used to detect resistance in other species are even longer. Approximately 10 days are required to detect antibiotic resistance in *Helicobacter pylori*, the bacteria responsible for gastritis and ulcers ^[14].

In order to shorten diagnostic time, polymerase chain reaction (PCR) protocols have been developed to diagnose antibiotic resistance. PCR is a procedure used to duplicate DNA molecules using short DNA primers and a thermal cycler. PCR methods have detected methicillin-resistant *Staphylococcus aureus* (MRSA) ^[15]. More recently, PCR methods successfully identified endodontic infections that were resistant to three commonly used antibiotics ^[16].

Despite recent successes, the current FDA approved PCR methods have their drawbacks: they require more sample preparation than desired, including a 24 hour blood culture, and eliminating the proteins in blood that inhibit PCR ^[17-19]. This is a challenge since proteins in blood outnumber the DNA molecules by a 4000 to 1 ratio ^[20]. In addition to complicated sample preparation, these methods also have a higher than desired limit of detection (LOD) of 10^6 colony forming units per milliliter (CFU/mL) ^[17].

Researchers have been able to diagnose infections without PCR or cell culture by using imaging techniques. One such study reported antibiotic resistance diagnosis in less than 30 minutes. In this method, bacteria were grown into micro-channels loaded with varying concentrations of antibiotics, and their growth was monitored by a camera ^[21]. However, the LOD was above 10^4 CFU/mL ^[21]. Thus, better methods to diagnose infections down to 10 CFU/mL still need to be developed.

1.3- Magnetic Microbeads for DNA Capture

Magnetic microbeads provide an important advantage for enriching DNA, because they can be manipulated using an external magnetic field, which will have no contact with fluid [22]. Protocols using magnetic microbeads have already been established to purify DNA and other biomolecules in many applications, including genome sequencing, enzyme purification, and cloning [22].

Magnetic microbeads have been used to extract small amounts of DNA in complex biological matrices. For example, microbeads were used for detecting circulating tumor DNA from human blood [23]. They also have been used to extract and enrich DNA that codes for a serious allergen in tomato plants without the use of PCR or cell culture [24]. Beads were also successfully used to enrich microbial DNA extracted from skin on a vertebrate host [25, 26].

The standard protocol for magnetic based DNA capture, shown in **Figure 1**, starts with a capture or “bait” sequence that is attached to the surface of beads. A complementary target ssDNA is captured by the modified microbeads during vortexing. After the beads are trapped by an external magnet, all other material is rinsed out so only the buffer solution, beads, and the captured DNA remain. A hybridization probe, tagged with a fluorescent molecule, will then flow past the beads and hybridize to the target sequence. The target DNA is detected by laser induced fluorescence after heating and elution [27, 28]. This process can enrich DNA samples from low concentrations, has high selectivity, and is compatible with automation [29].

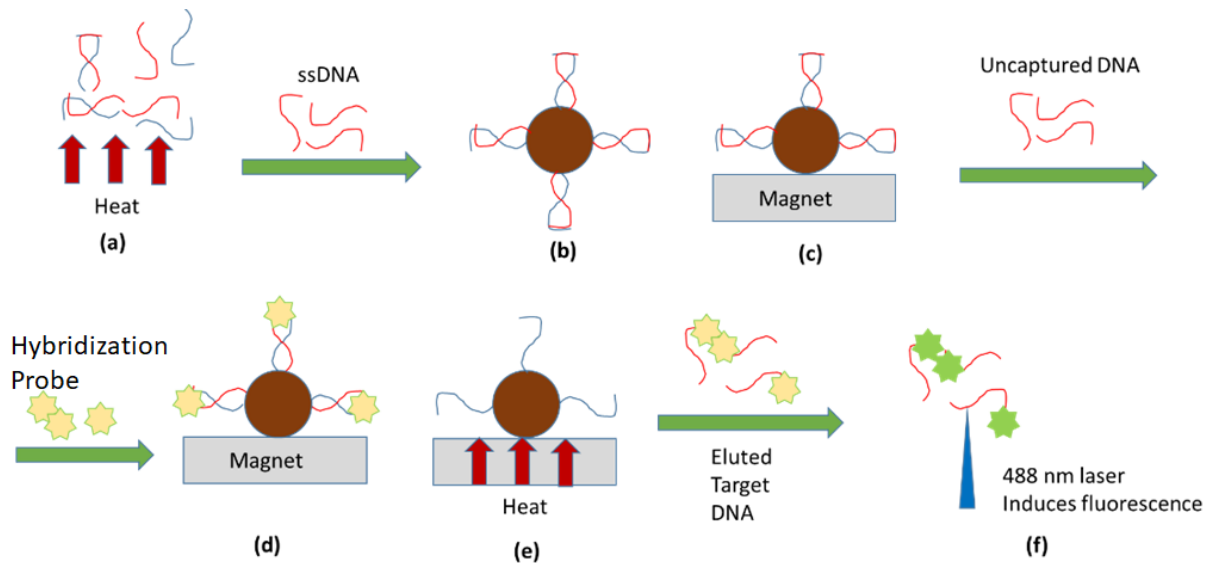


Figure 1- Standard process for denaturing, capturing and labeling DNA. **(a)** Double stranded DNA is denatured by heating to 90 °C. **(b)** Target DNA hybridizes with ssDNA attached to the beads. **(c)** Beads with hybridized DNA will be pulled down by a magnet as all other DNA is rinsed through. **(d)** DNA hybridization probe with fluorescein attached will hybridize with the target DNA on the beads. **(e)** After heating DNA will de-hybridize and flow past a **(f)** focused 488 nm laser, inducing fluorescence and allowing the DNA to be detected.

Many researchers carry out the procedure described in **Figure 1** in centrifuge tubes ^[27], which is useful in a laboratory, but not in a point of care setting. Centrifuge tubes require more handling since the tube needs to be moved from one piece of hardware to another, such as from a vortexer to a centrifuge. The need for human intervention in this system makes it costly and time consuming. The preferred method is an automated system in which extraction, mixing, elution, and detection are integrated in one device ^[30]. Automated systems can increase efficiency of analysis by eliminating the need for repetitive steps, and reducing human error, and increasing the consistency of the results ^[31].

1.4- Microfluidics

Microfluidics are defined as systems in which fluid flow behaves differently from conventional flow, due to small dimensions [32]. The small scale increases the surface to volume ratio, and allows for laminar flow [33]. A key advantage of using microfluidics is that their closed off nature makes it possible to integrate multiple laboratory operations in one device, allowing for analysis to continue uninterrupted [32, 34]. This feature alone makes microfluidics advantageous in food science, medical devices, and in chemical industries [33].

In order to work effectively, microfluidics need to be enclosed. Two common ways to seal the channels of microfluidics are thermal treatment [35], or using pressure sensitive adhesives (PSAs) [36]. PSAs bond planar materials together through thin adhesive layers [37]. Due to their versatility, PSAs have been included in a number of microfluidic devices [38].

Microfluidics can be used to separate and isolate molecules that are present in minute concentrations [32]. To enhance these abilities, integrating devices with magnetic microbeads is common [22]. However, most of the protocols for magnetic microbeads involve turbulence, but microfluidic flow is laminar [39]. To mix in the absence of turbulence, magnetic microbeads in the channel need to be agitated [39-41]. To solve this problem, studies have been done to agitate magnetic particles in laminar flow using external magnetic fields [42].

1.5- Microfluidic DNA Capture with Magnetic Microbeads in Sepsis Diagnosis

This thesis is part of a broader project to develop a system with the goal to purify and identify antibiotic resistance genes in less than one hour using only 7 mL of blood, as depicted in **Figure 2**. Upstream from my work, bacterial cells will be separated from blood, lysed, and then their DNA collected [43, 44]. Downstream from my work, optofluidics, technology that integrates

optics, femtoliter volumes, and optical waveguides, will be used to achieve single molecule DNA detection [45, 46]. Using multiplexing, DNA molecules of multiple sequences will be detected simultaneously [47].

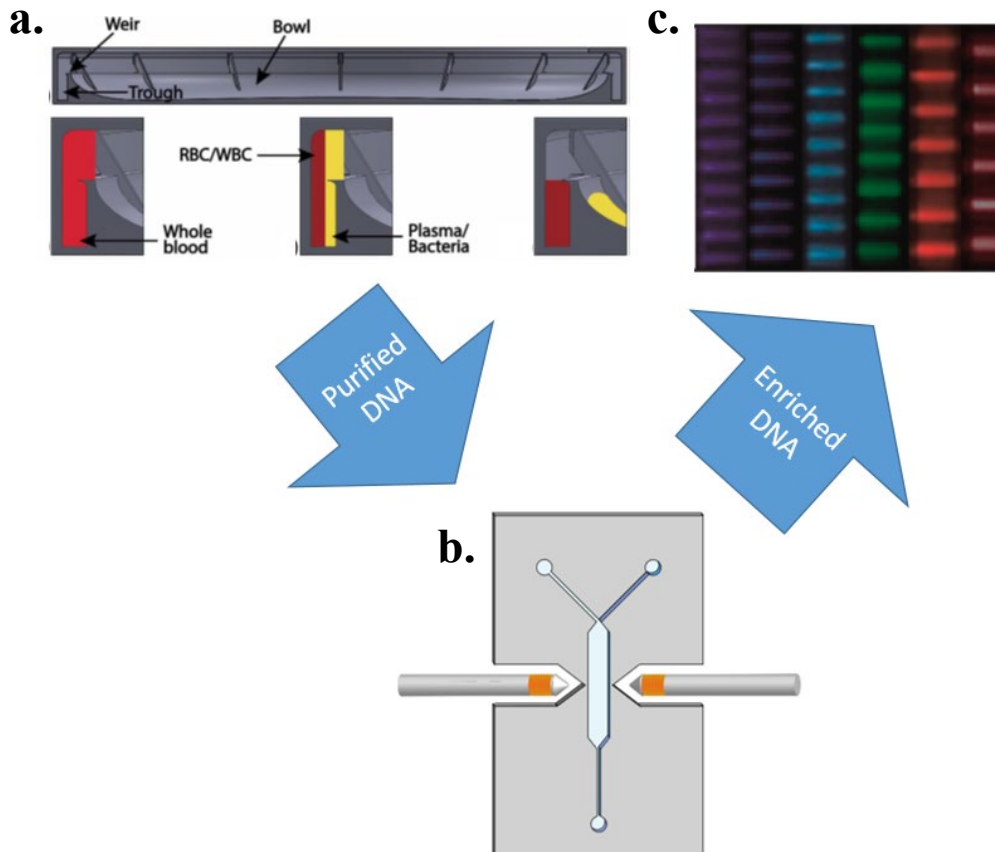


Figure 2- The process of isolating, enriching, and detecting minute concentrations of DNA extracted from human blood. **a.-** Bacteria are separated from blood, lysed and then their DNA is extracted [43]. **b.-** Magnetic microbeads are used to enrich the target DNA to detectable levels **c.-** Optofluidics, with single molecule sensitivity, will be used to detect multiple gene sequences [45-47].

Symptoms can be manifest in a patient with a concentration as low as 5 CFU/mL in human blood [4], so low levels need to be detected, and a high percentage of bacteria needs to be recovered. To increase capture yields of bacteria, Dr. Pitt's group developed a centrifuge system, where after spinning at 3000 rpm for one minute, red and white cells would sediment while bacteria would remain suspended in the plasma [48].

After extraction, the bacteria were lysed in 6 M guanidine HCl and 0.5% (w/v) SDS in 10 mM Tris-HCl for 5 minutes at room temperature ^[49]. To extract DNA, silica coated magnetic microbeads were vortexed with the mixture for 30 seconds in a micro-centrifuge tube ^[49]. After beads were trapped with a permanent magnet, supernatant was removed and the beads were washed with buffer ^[49].

The centrifugation process had 58% recovery of bacteria from the spiked blood ^[49]. The amount of purified double stranded DNA recovered was 0.4 ng/ μ L ^[49]. This recovered DNA is the planned input for my DNA capture system.

A colleague in my lab, Radim Knob, developed a process to take this purified DNA, and enrich and label it using a microfluidic device with an integrated monolith, a porous polymeric column modified with oligonucleotides complementary to the target DNA ^[49]. The schematic of the device is shown in **Figure 3**. This device included a serpentine channel, directly under a denaturing heater that was set to 90 °C ^[49]. Once denatured, the resulting ssDNA flowed through the monolith, hybridized with the attached DNA, and was labeled with a fluorescently tagged oligonucleotide ^[49]. After heating and elution, the DNA was detected by laser induced fluorescence ^[49]. The process detected sepsis related DNA from blood with a LOD < 1 pM ^[49].

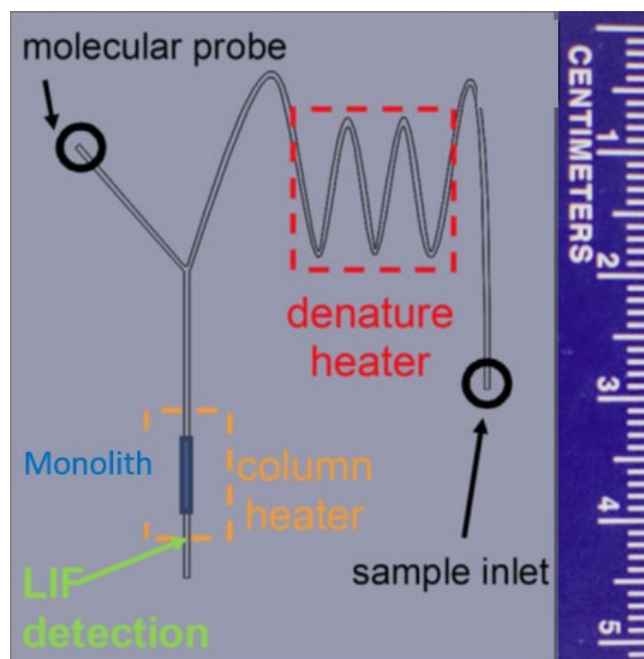


Figure 3- Schematic for microfluidic chip for DNA capture. Double stranded DNA is introduced in the sample inlet and denatured in the serpentine channel, and the resulting ssDNA fragments are captured on the monolith. After heating, the DNA flows past a laser detector ^[49].

To enrich DNA, I use a similar procedure, but instead of a monolith, I use magnetic microbeads. Magnetic microbeads have an advantage over monoliths in that they are mobile in external magnetic fields ^[22, 33]. This allows for suitable capture efficiency without the backpressure produced by monoliths ^[50].

After enrichment of DNA, it is sent to UC Santa Cruz for optical detection of multiplexed, fluorescently labeled DNA. They previously demonstrated the concept of using simultaneous detection of multiple particles in determining three different virus strains, and different DNA sequences of the Ebola virus ^[47, 51]. In these systems, different molecules were labeled with unique fluorophores that excite at specific wavelengths. By using a multimode interference (MMI) waveguide, wavelength dependent spot patterns were created in a single microfluidic channel ^[47]. This allowed for each fluorophore associated with each individual

molecule to be excited under its specific wavelength ^[47]. This system was sensitive enough to detect DNA molecules without any amplification ^[51].

1.6- Summary of Thesis Work

In Chapter 1, I summarized different methods of detecting antibiotic resistant DNA. The advantages of using microfluidics and magnetic microbeads were described. In my thesis, I investigate these further to improve the capture efficiency of DNA.

In Chapter 2, I discuss experiments I have done using magnetic microbeads in micro-channels. Fluorescently labeled DNA is loaded in a channel along with magnetic microbeads in different flow conditions. I describe results of testing different bead and DNA loading conditions. Results for DNA capture and labeling in a channel are described.

Chapter 3 discusses the use of PSAs and magnetic mixing. Different PSAs were tested for fluorescence to determine which ones were most suitable. The best PSAs were formed into a mixing well laser cut from PMMA. The mixing wells were loaded with a magnetic bead suspension, and subjected to different magnetic field conditions, and the capture efficiency of fluorescently labeled DNA was compared.

Chapter 4 discusses the conclusions from these experiments, which suggest that DNA capture efficiency can be improved further. The future work section includes possible ways to make these improvements.

2. DNA CAPTURE, ENRICHMENT AND DETECTION USING MAGNETIC MICROBEADS IN MICROFLUIDIC CHANNELS

2.1- Introduction

In order to improve DNA capture efficiency of magnetic microbeads in a microfluidic setting, different flow conditions need to be tested. This chapter compares the results of DNA capture in different laminar flow conditions, to determine what conditions have the best capture efficiency. To evaluate capture efficiency of ssDNA on magnetic microbeads, three different experimental approaches were tested: 1. Co-flow, where beads and DNA were flowed in a channel at the same time, 2. Packed bed, where particles were deposited first and DNA flowed through the resultant porous bed, and 3. Pre-mixed, where beads and DNA were vortexed in a centrifuge tube before being introduced in the channel. This chapter outlines the experimental procedures of each method, along with the results and conclusions.

2.2- Experimental

Magnetic microbeads coated with streptavidin were purchased from New England BioLabs and modified with a biotinylated ssDNA capture sequence, shown in **Table 1**. Before beads were modified they were rinsed 3 times with buffer. Between each rinse, a permanent magnet would pull down the magnetic beads and the supernatant was removed with a pipette. After rinsing, the beads were suspended at a concentration of 1 mg/mL in a buffer solution composed of 100 nM ssDNA, 50 mM MgCl₂, 500 mM NaCl, and 20 mM Tris-HCl, pH 8. The resulting mixture was vortexed and incubated at room temperature for 30 minutes.

After modification, the beads were ready to capture the target sequence. The target was a 90 mer ssDNA molecule originating from the *Klebsiella pneumoniae* Carbapenemase (KPC) antibiotic resistance gene, labeled with fluorescein, as shown in **Table 1**.

Table 1- DNA capture and target sequence for the KPC antibiotic resistance gene.

Capture sequence	Target sequence
Biotin- TATCGCCGTCTAGTTCTGCTGCTTG	CATTCAAGGGCATCTTTCCGAGATGGGTGACCACGGAACCAGCGG ATGCCCATGCCCTATCAGTCAAGACAGCAGAAGTAGACGGCGATA

A polypropylene chip with a Y shaped channel was the primary device used in testing. The fabrication of the chips required the use of an engraved aluminum plate and a hot press. Channels were 200 μm wide and 500 μm deep. The engraved aluminum plate and a polypropylene piece were placed between two glass slides and inserted in a Carver Hot Press. The press had two plates that were 30.5 x 30.5 cm, and had the maximum force equivalent to 12 tons. Each plate of the hot press was set to 150 $^{\circ}\text{C}$. After applying between 5.5-6.7 MPa on the assembly, it sat at that pressure for 90 seconds. Once the pressure was released, the piece with the embossed design was placed with fresh glass slides and allowed to cool while pressed between two copper plates. After cooling, the chip was sealed with a transparent polypropylene film in the hot press at 147 $^{\circ}\text{C}$ by applying between 0.6-1.4 MPa for 1-20 seconds. A finished device is shown in **Figure 4**.



Figure 4-A typical polypropylene chip with a Y channel.

A typical experiment used a 30 $\mu\text{L}/\text{min}$ flow rate that was controlled by a Fluigent pump system. Pre-labeled DNA (1 nM) flowed in one branch of the Y, while DNA modified beads (1 mg/mL) flowed in the other branch. The capture sequence on the beads would hybridize with the target sequence in the main channel.

In order to control the temperature, an input wire was affixed to the bottom of the chip flush with a permanent magnet, 6 mm in diameter and 3 mm thick, (Amazing Magnets, Inc.). A control wire was placed directly above the input wire which was flush with a TE Technology ceramic, potted heater (Figure 5). This allowed temperature control where the beads were captured. To detect eluting DNA, a 488 nm laser, focused 2 mm beyond the magnet, induced fluorescence of the fluorescein-labeled target DNA. The resulting fluorescence was recorded digitally by a National Instruments LabVIEW program.

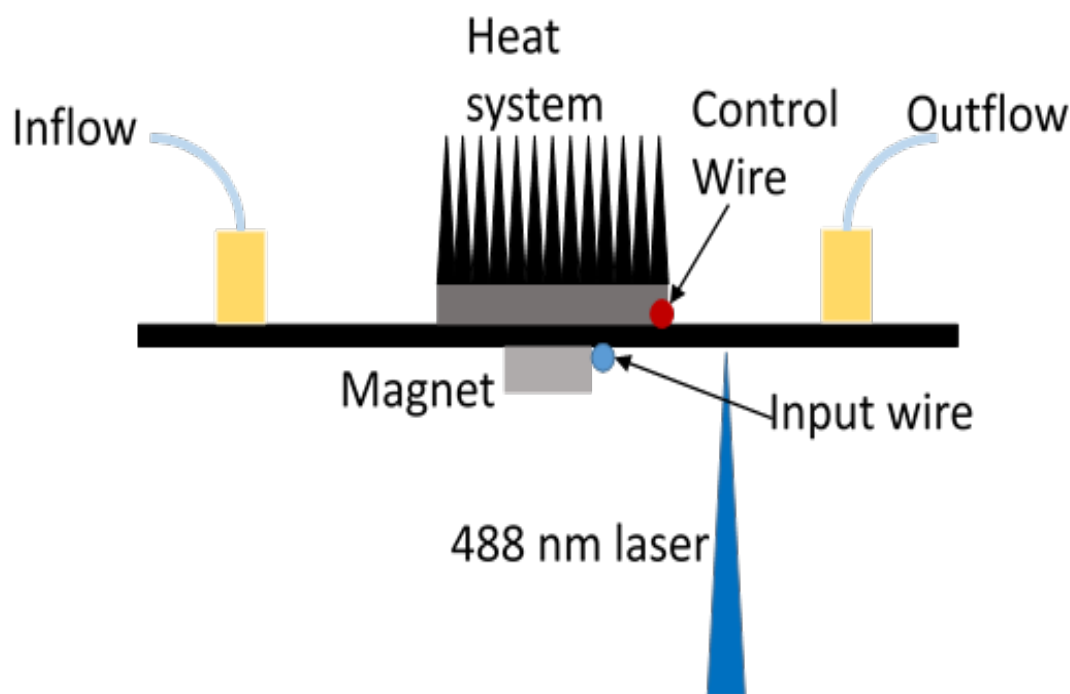


Figure 5-Schematic depicting the experimental setup for a DNA capture and elution experiment. The inflow includes DNA and microbeads. The beads are trapped by the permanent magnet and all other material washes through. After heating, the released DNA is detected by fluorescence from the 488 nm laser excitation.

Before DNA capture experiments were performed a calibration was made to determine what peak heights were associated with what concentrations. This was done by flowing 100 μL of solutions of 1-5 nM fluorescently labeled DNA through the channel. This procedure was repeated for every capture experiment, because the peak values varied between different channels.

The process of capturing the DNA for these experiments was similar to the procedure described in **Figure 1**, except fluorescein was already attached to the DNA molecules, as shown in **Figure 6**. This eliminated the extra variable associated with labeling.

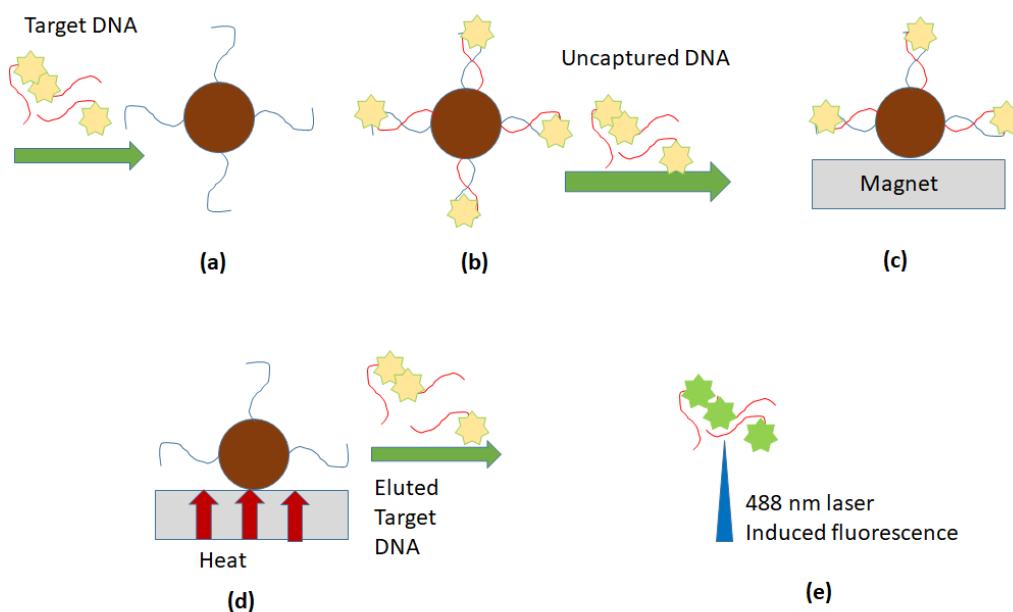


Figure 6- Standard process for capturing and enriching pre-labeled DNA. **(a)** Target DNA flows past magnetic beads, modified with a ssDNA complementary to the sequence of interest. **(b)** ssDNA complementary to the DNA on the bead will hybridize, and all other DNA will not. **(c)** Magnetic beads with captured DNA will be pulled down by a magnet as all other DNA is rinsed through. **(d)** After heating, DNA will de-hybridize and flow through the channel. **(e)** The DNA will flow past a focused 488 nm laser, inducing fluorescence and allowing the DNA to be detected.

For co-flow experiments, 1 nM of fluorescently labeled DNA flowed in the channel along with a 1 mg/mL bead suspension. When 60 μL of the bead suspension had flowed through the

channel, the flow was turned off, the capture region was heated until the temperature reached 65 °C, and then the flow was turned back on after two minutes. The resulting peak heights were compared to the calibration curve to determine concentration.

The second set of experiments involved packed bead beds. This was done by flowing 60 μL of 1 mg/mL bead suspension the channel at 30 $\mu\text{L}/\text{min}$ for 2-3 minutes. The beads were trapped by a permanent magnet at the bottom of the channel forming a packed bead bed. 100 μL of 1 nM DNA was flowed through this bed at 30 $\mu\text{L}/\text{min}$. After heating the capture region at 65 °C for two minutes the flow was turned back on and the captured DNA eluted past the detector.

Modified beads with pre-hybridized DNA were used in the third set of experiments. The beads (1 mg/mL) were combined with 200 μL of 1 nM target DNA, vortexed and incubated at room temperature for 10 minutes before being introduced in the chip. 60 μL of the modified beads were loaded in one branch of the Y channel, while buffer solution was introduced in the other. The beads were captured during flow. DNA was then eluted and detected as in the previous experiment.

The fourth set of experiments involved on-chip denaturing, capture, labeling and elution, as described in **Figure 1**. The chip design used for these experiments is similar to that in **Figure 3**. 10 nM dsDNA was loaded into the right entry port so it would flow through the serpentine channel. Simultaneously, microbeads were loaded into the left entry port and were trapped by the permanent magnet before interacting with the DNA. DNA was denatured at 90 °C as it flowed through the serpentine channel, and the resulting ssDNA was captured by the magnetic beads. After the beads were trapped by the permanent magnet, a labeled complementary DNA sequence was loaded in the left entry port, where it flowed through the packed bead bed and

hybridized with the captured DNA. After the same heating and elution procedure described above, the labeled DNA was detected by laser induced fluorescence.

2.3- Results

Figure 7 shows the results of a calibration curve experiment. The signal corresponding to each concentration was considered to be the point where the signal plateaued, e.g., the region between 1000 seconds to 1500 seconds for 2 nM. The spikes immediately following the broad plateau are the result of flow from both channels being turned on to flush out the fluorescent solution. In this particular experiment 1 nM of labeled DNA yielded a signal of approximately 0.6 V, 2 nM yielded approximately 0.8 V, and 3 nM yielded approximately 1 V. The resulting calibration curve had the formula of $c = 0.645 V$. Higher flow velocities generally resulted in higher signals.

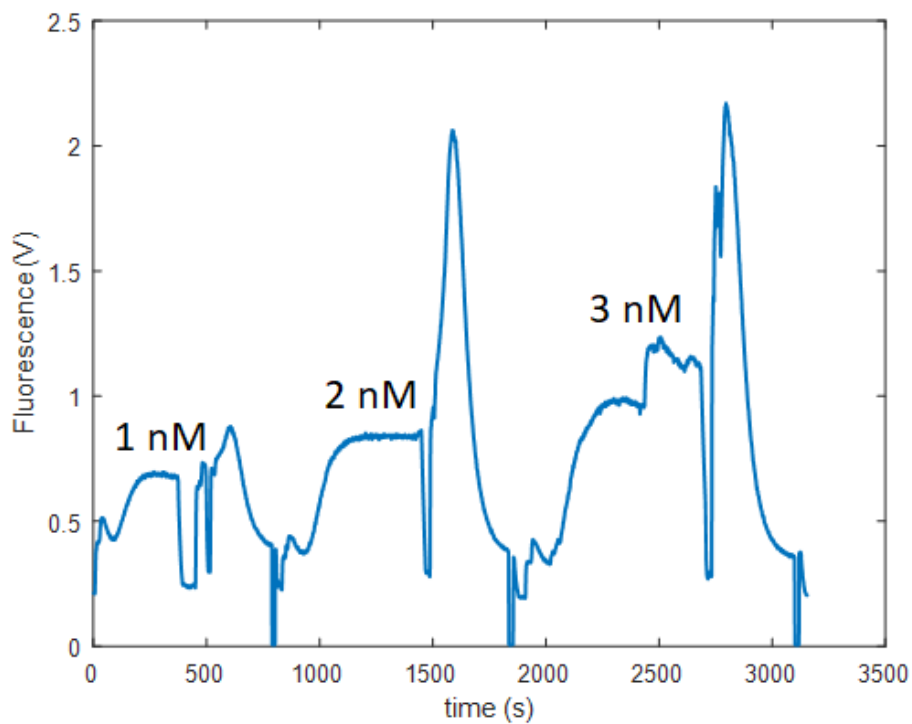


Figure 7- Calibration curve for an on-chip experiment using three different DNA concentrations.

Figure 8 depicts fluorescence results obtained for a co-flow experiment. The signal started high when buffer was first loaded in the chip, but after photobleaching, the signal reached background levels around 400 seconds. DNA and beads were flowed at 500 seconds, and the rise in signal between 600 to 1200 seconds was due to the uncaptured DNA flowing past the laser. Flow was stopped at 1200 seconds resulting in a lower signal. An elution peak immediately appeared at 1600 seconds after flow was turned back on. Repeating the co-flow procedure 12 times yielded elution peaks with an average height of $0.90 \text{ V} \pm 0.60 \text{ V}$.

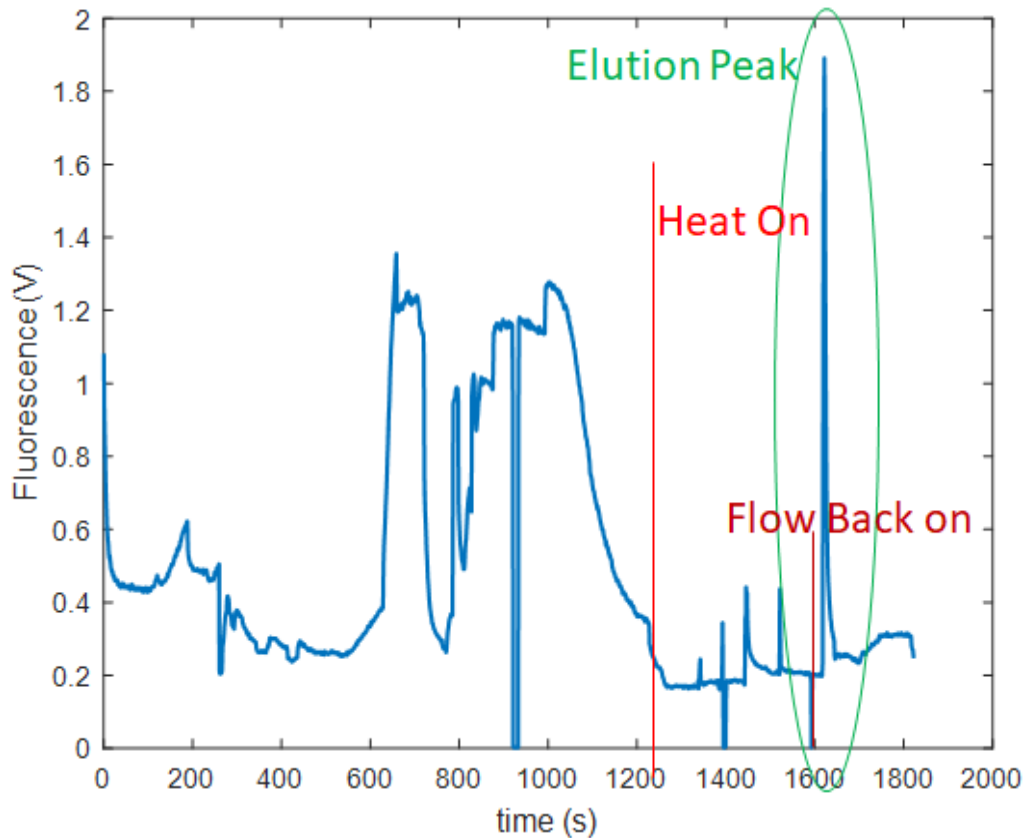


Figure 8 – Fluorescent signal as a function of time during loading, capture and elution of 1 nM fluorescently labeled DNA. For this experiment beads and DNA flowed in the channel simultaneously.

Figure 9 depicts fluorescence results for a packed bead bed experiment. In this experiment, the recording started after the beads were loaded and captured by a magnet. From 0 to 600 seconds, 1 nM of DNA was being flowed through the channel and uncaptured DNA was detected. The flow was turned off at 600 seconds and the heat was turned on. A spike at 900 seconds is due to a flashlight error. Flow was turned on at 950 seconds and an elution peak appeared immediately afterwards. Repeating the packed bead bed procedure 6 times yielded elution peaks with an average height of $0.66 \text{ V} \pm 0.50 \text{ V}$.

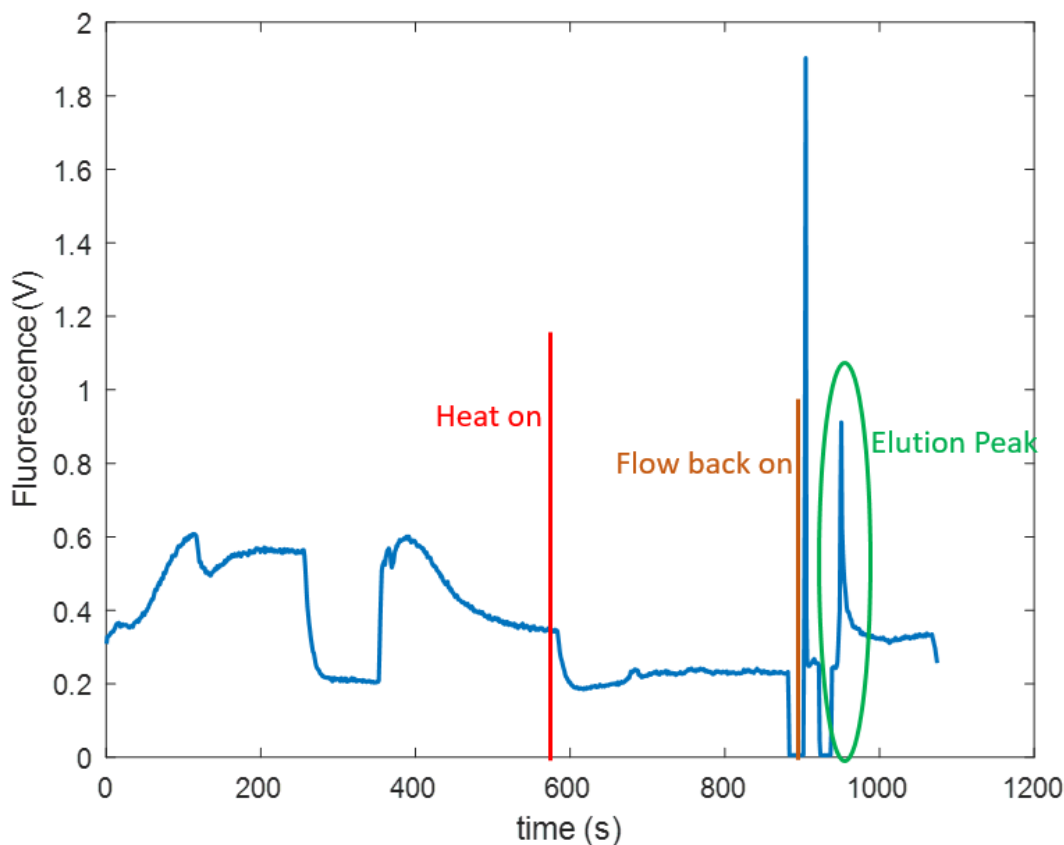


Figure 9- Fluorescent signal as a function of time during loading, capture and elution of 1 nM fluorescently labeled DNA. Beads formed a packed bed before DNA flowed through the channel.

Figure 10 depicts fluorescence results for a pre-hybridization experiment. Between 0 to 500 seconds, the beads modified with attached fluorescently labeled target sequence were flowed

through the channel. There was no increase in signal because all of the fluorescently labeled DNA was attached to the beads that were trapped by the permanent magnet. After heating at 65 °C for two minutes, the flow was turned on at 1050 seconds and a sharp elution peak appeared. Repeating the pre-hybridized bead procedure 12 times yielded elution peaks with an average peak height of $1.7 \text{ V} \pm 1.4 \text{ V}$.

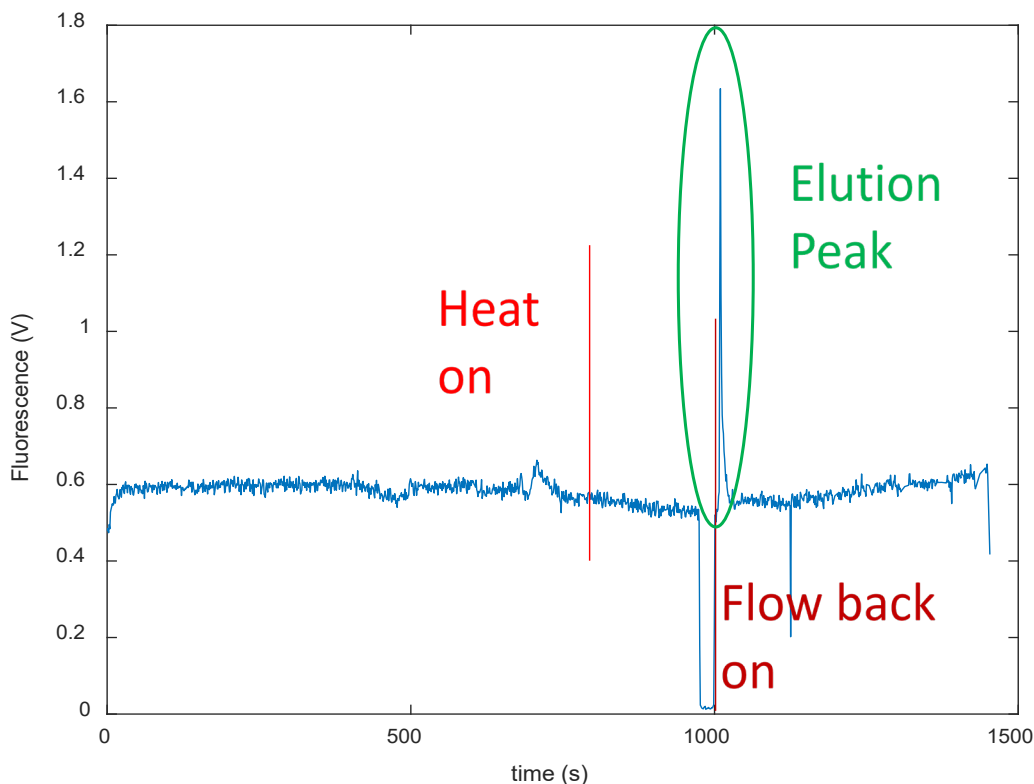


Figure 10- Fluorescent signal as a function of time during an experiment where 1 nM of fluorescently labeled target DNA was pre-hybridized with the capture sequence on the beads before being introduced in the channel.

After consistent results were achieved with pre-labeled DNA, I carried out on-chip denaturation of unlabeled dsDNA followed by hybridization, fluorescence labeling, and elution. Fluorescence results are shown in **Figure 11**. In this graph, the signal between 0 to 500 seconds, is due to DNA and beads being loaded into the device. Flow was then turned off at 500 seconds

resulting in a drop in signal after 600 seconds. The increase in signal at 1200 seconds was due to uncaptured hybridization probe flowing past the laser. Flow was turned off at 2000 seconds while the capture region was heated. A sharp elution peak appeared when flow was turned on at 2600 seconds. This procedure was performed three times and yielded an average peak height of 2.12 V and a SD of 0.90.

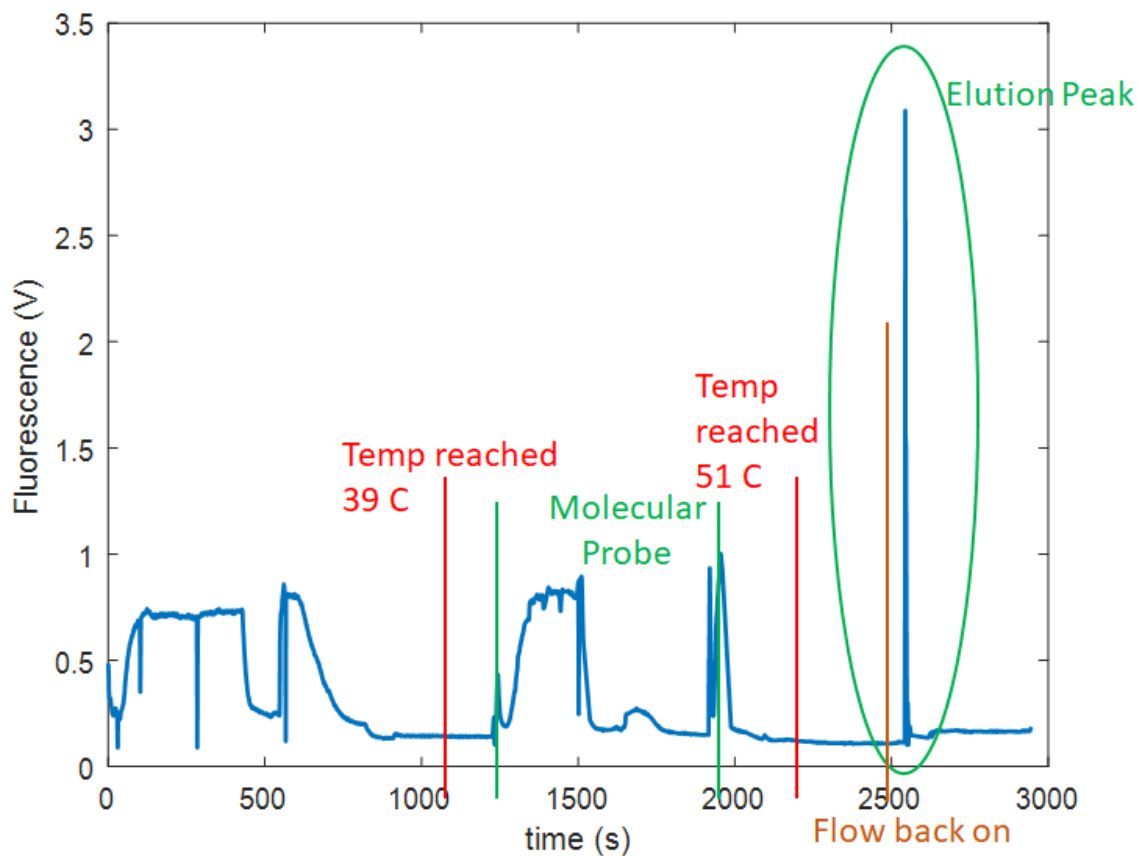


Figure 11- Fluorescent signal as a function of time during an experiment where 1 nM of unlabeled dsDNA was de-hybridized, then captured and labeled on beads localized in a channel, and eluted.

By performing a *t*-test, the means of the elution peak heights for the co-elution and pre-hybridized experiments were determined to be significantly different at the 95% confidence level. The peaks for the pre-hybridized beads were higher, indicating that more DNA was

captured in this method than in co-elution. This means that mixing or agitating the beads to capture DNA increases signal.

A *t*-test comparing the means of the elution peak height for the co-elution and packed bead bed experiments showed no significant difference at the 95% confidence level. Another observation made was the frequency of elution peaks. In every iteration of the co-elution method, an elution peak was observed. Only half of the packed bead bed experiments had an observable eluted peak. This indicates that co-elution is more reliable than packed bead bed.

After measuring peak heights, the concentrations of eluted DNA were calculated from the peak heights and calibration curves; the results are shown in **Table 2**. The results show that pre-hybridization not only increases signal but also increases concentration. Because pre-hybridization involved mixing of beads with DNA, I conclude that mixing is a way to improve DNA capture.

Table 2- The average peak heights and estimated concentrations for each method. 1 nM was the loaded concentration for all experiments.

Method	Average Peak Height (V)	Peak Height SD (V)	Average Concentration (nM)	Concentration SD (nM)
Pre-hybridized with Labeled DNA	1.7	1.4	2.7	2.4
Co-Flow with Labeled DNA	0.68	0.51	0.53	0.64
Packed Bead Bed with Labeled DNA	0.67	0.49	0.76	0.76
Fluorescently Labeled in Channel	2.12	0.90	7.3	4.4

2.4- Discussion

In theory, the packed bead bed would be expected to be the best method due to tortuosity, and increased probability of intermolecular interactions. This means that the signal should be low when fluorescently labeled DNA is flowed through the channel, and the elution peak should be high, but this was not the case. SEM images showed, that instead of filling up the channel, the beads aggregated into brick-like structures in some areas, as shown in **Figure 12**. This meant that the majority of the DNA could flow through the channel without passing through the aggregated beads.

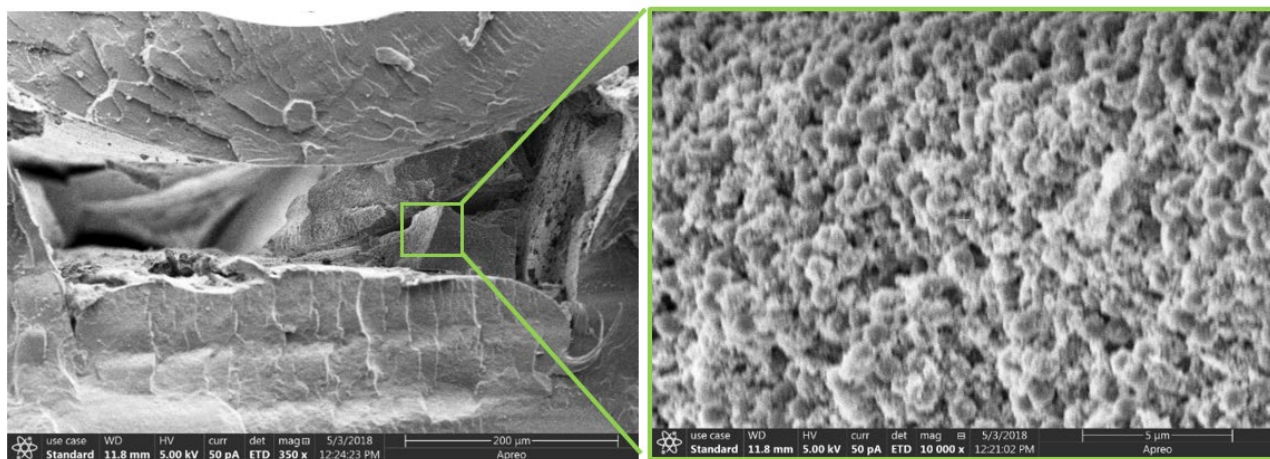


Figure 12-SEM image of magnetic microbeads aggregated in a channel (left), and a zoomed in image of the boxed area (right). This image shows, that instead of filling the entire channel, the beads aggregated in brick-like structures.

Laminar flow of beads and DNA through a straight channel is not a reliable condition for bead-based DNA capture based on the results for the co-flow experiments. In theory, diffusion should be the driving mechanism for DNA hybridization since there is no turbulence. However, the channels would have to be much longer for diffusion to take full effect. The diffusion coefficient of 100 bp DNA in buffer being $21 \mu\text{m}^2/\text{s}$ ^[52], which means that it would take approximately 5952 seconds, or 1 hour and 40 minutes for DNA to diffuse 500 μm , the channel

size of my device ^[52-54]. Time constraints on the assay limit how much diffusional mixing occurs.

Pre-hybridizing the beads in a centrifuge tube before flowing them in a channel allowed for better enrichment of DNA, because the beads were agitated in the solution allowing for more interactions with DNA. The results of the pre-hybridized experiments show that mixing with beads is crucial but not achieved well in laminar flow.

A reason for variations in fluorescent signal between devices was the attachment of the transparent polypropylene film. When overheated, the film would sink in the channel, lowering the channel height. When underheated, the film would delaminate when pressure was applied, allowing fluid to leak out of the channel. Both scenarios altered the signal. Since I was unable to adhere the transparent polypropylene to the chip in the exact way every time, alternate device fabrication strategies became attractive.

2.5- Conclusion

My results show that there was no significant difference between the packed bead bed method or co-flow. However, in the pre-hybridized bead experiments, DNA capture was greater. Because the pre-hybridized experiments worked the best, it is necessary to explore methods that involve mixing. This led me to explore the use mixing wells and electromagnets to induce bead movement.

3. FABRICATION OF ELECTROMAGNETIC MIXING CHAMBERS USING PRESSURE SENSITIVE ADHESIVES

3.1- Introduction

The experiments described in **Chapter 2** revealed that mixing and agitating the magnetic beads resulted in greater amounts of captured DNA, so a microfluidic method of mixing is desirable. Also, to have more consistent fluorescence signals, a better device assembly is needed. Thus, the use of PSAs and electromagnets was explored to increase DNA capture and improve consistency.

This chapter describes the selection of the best PSA for flow through experiments, and the fabrication of the mixing wells. It also describes operating electromagnets at different frequencies to determine what frequency leads to greatest DNA capture. With the right device geometry and frequency settings, capture efficiency of the beads was improved.

3.2- Experimental

I first set out to select the best PSA for experiments in detecting fluorescently labeled DNA. I obtained a sample kit from 3M containing seven transparent PSAs, along with a double-sided adhesive. One factor in selecting a PSA was the auto-fluorescence, which should be in the same range of that of polypropylene. Device fluorescence should be sufficiently low that 1 nM fluorescently tagged DNA would emit a signal well above the device background. The PSAs that had sufficiently low auto-fluorescence were then tested for temperature stability and mechanical strength. The different polymers tested are listed in **Table 3**.

Table 3- 3M polymers that were evaluated.

Polymer name	Adhesive Type	Material
9984	none	Polyester
9969	Acrylic	did not say
9964	Acrylic/Acrylate	Polyester
9962	none	Polyester
9960	none	polyester
9795R	Silicone Acrylic	polyolefin
9793R	Acrylic/Acrylate	Polyolefin

To test the auto-fluorescence, channels were imprinted into black polypropylene using the same procedure described in **Section 2.2**. For the polymers that did not have an adhesive side, a channel was cut out of a piece of 9965 double-sided adhesive, which was then placed on the polypropylene surface (see **Figure 13**). The transparent film was then layered on top of the 9965. Adhesive polymers were placed directly on the polypropylene surface.



Figure 13- A channel cut out of white 9965 double-sided adhesive that was placed directly above an imprinted channel with a 9969 layer. Different films were layered on top of 9965 for auto-fluorescence experiments.

A 488 nm laser was focused in the middle of the channel as buffer flowed through at ~30 $\mu\text{L}/\text{min}$. The experiment was run for 10-60 minutes and the fluorescence was measured at the start and at the end.

Besides fluorescence, I also tested for heat resiliency. I did this by taping the heating wires directly to the polymer adhering it to a solid substrate, and raising the temperature to 90 °C

for 3 minutes. If the polymer did not warp and stayed adhered to the substrate, it was considered a suitable polymer to use.

Mixing chambers were fabricated by cutting channels out of PMMA using a CO₂ laser from VersaLaser, and sealing them over with a PSA. Experiments were done using two different reservoir designs as shown in **Figure 14**. The circular wells were 6 mm in diameter and 100 μ m deep. The diamond wells were 6 mm long, 1 mm wide, and 100 μ m deep. 1 mm diameter holes were cut directly above each well to insert the bead suspension and DNA solution into the mixing chambers. The distance between holes was 4 mm for the circular wells and 6 mm for the diamond wells. After cutting, each device was sealed over with a 9793R PSA.

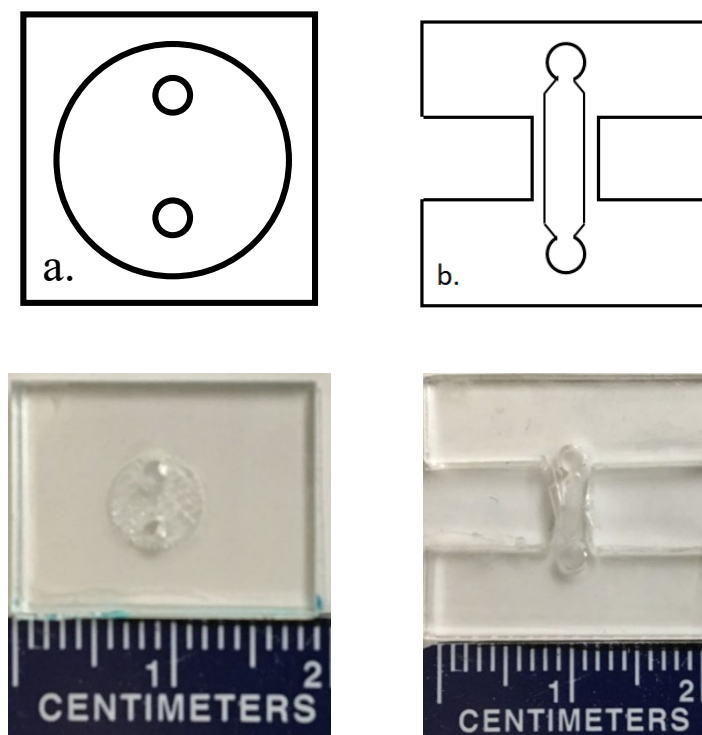


Figure 14-Wells used for electromagnetic mixing chambers **a.**- A circular well in PMMA, **b.**- A diamond shaped well.

Once the wells were sealed, they were placed between two copper electromagnetic coils from Mouser Electronics. The coils had a 6 mm outer diameter, a 4 mm inner diameter, and a 4

mm length. The core of the coil was either an iron roofing nail (2.54 cm long) for the diamond wells, or a 4 mm diameter iron cylinder for the circular wells.

A set of experiments was performed to determine if an AC electromagnetic field affected DNA capture efficiency. To test this variable, the circular wells were placed firmly between two cylindrical electromagnets as shown in **Figure 15**.

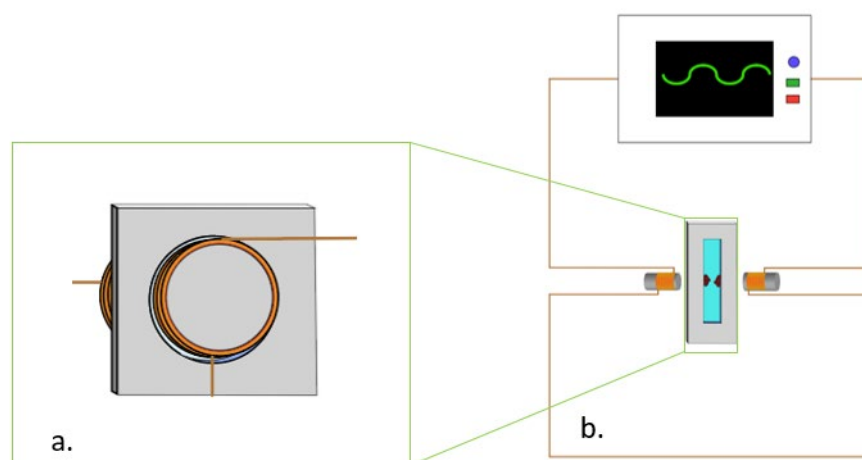


Figure 15-Two electromagnets connected in series with a mixing in between **a.**- Top view of a well with electromagnets placed directly above and beneath. **b.**-Side view of a well with electromagnets connected in series with a signal generator.

The signal generator was set to a square wave pattern of frequencies 0 Hz, 50 Hz, and 100 Hz with an amplitude of 5 V. A 50 nM DNA solution was prepared, its RFU value was measured with a Thermo-Fisher NanoDrop 3300, and then the DNA solution was mixed with the magnetic beads (1 mg/mL). After subjecting the DNA/bead mixture to an electromagnetic field for five minutes, the DNA solution was extracted from the device and a new RFU value was measured and subtracted from the initial value to obtain a Δ RFU value. The Δ RFU values were compared to the Δ RFU from an experiment where beads and DNA were agitated in a centrifuge tube, as described in **Section 2.2**.

I also evaluated the diamond shaped wells using an AC electromagnet with permanent magnets attached. Roofing nails were used in place of the cylindrical cores for the electromagnets. At the head of each nail was 6 mm diameter, 3 mm thick neodymium magnet, placed so both north poles faced inward. It was hypothesized that tips of the nails would focus the magnetic field to a narrower area creating a stronger force. The experimental design schematic is in **Figure 16-a**, and a photograph of the electromagnets is shown in **Figure 16-b**. The signal generator frequencies tested for this experiment were 2 Hz, 50 Hz, 100 Hz, and 500 Hz. The same DNA concentration, wave pattern, and amplitude as in the circular well experiments were used for this experiment. The results were compared with a vortex experiment and a 0 Hz control.

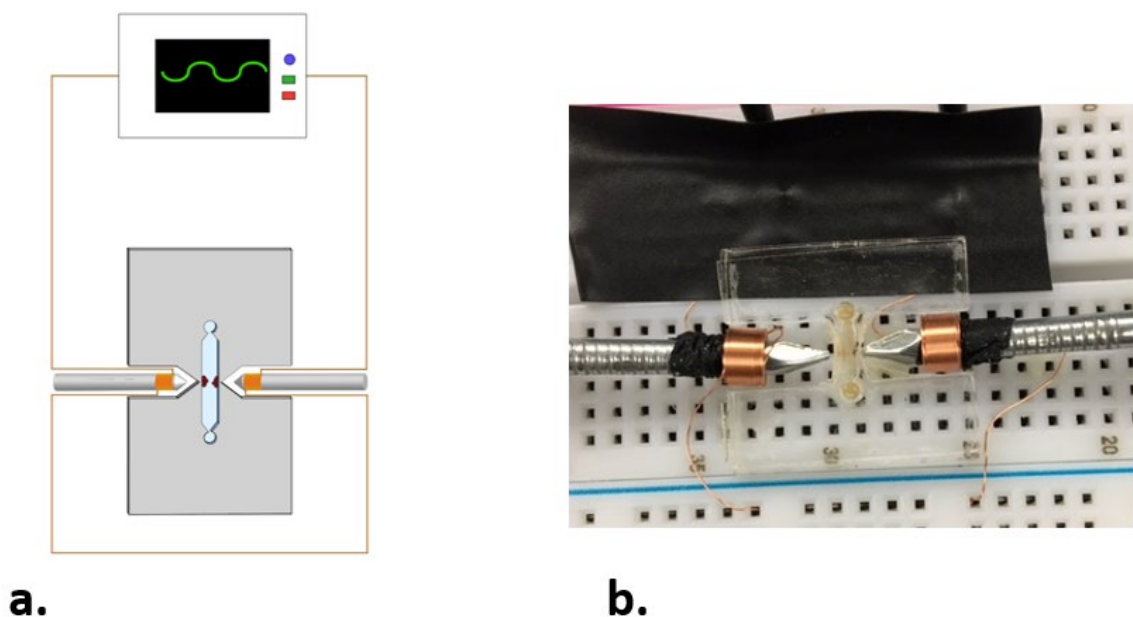


Figure 16- Capture electromagnets connected in series with an AC generator. **a.-** Schematic of the well, AC magnets and generator. **b.-** Photograph of the two AC magnets on each side of the mixing well.

To automate experiments, an Arduino Uno chip was used instead of a signal generator. Each electromagnet was connected to its own MOSFET transistor which was connected to a pin

on the Arduino chip. The general arrangement of the electromagnets, the transistors and Arduino chip is shown in **Figure 17**. A detailed wiring schematic of all the components and wires is given in **Figure A.1** in **Appendix A**.

Control experiments were done in vortexed centrifuge tubes and in a well without a magnetic field applied. The other conditions tested included 100 Hz symmetric (where both electromagnets are turned off and on simultaneously); 100 Hz asymmetric (where one electromagnet is off while the other is on, with or without a permanent magnet); and a signal generator experiment for comparison. All experiments used a square waveform at an amplitude of 5 V.

For the Arduino chip experiments, a 50 nM DNA solution was used, and beads (1 mg/mL) modified with 1 μ M capture DNA were used.

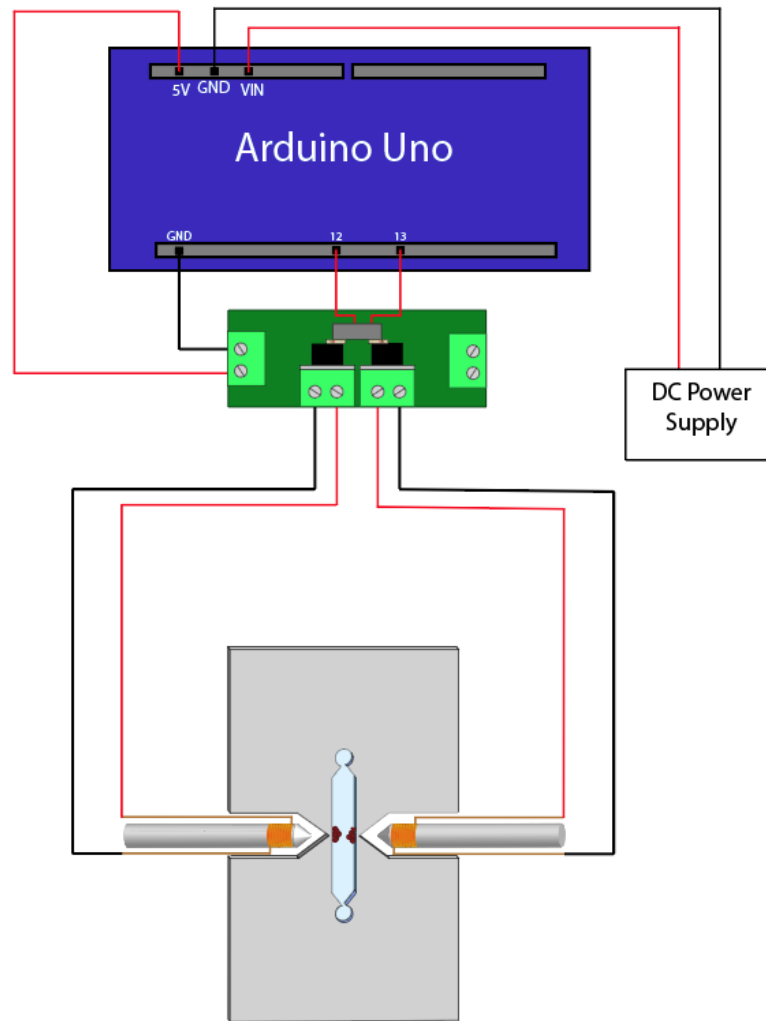


Figure 17- General arrangement for Arduino based mixing experiments. The electromagnets were placed on either side of the mixing well, and were turned on in a pattern controlled by the chip.

3.3- Results

Table 4 shows the results of the auto-fluorescence tests for each polymer. 9793R and 9795R were the two polymers with the lowest initial fluorescence signal, and the lowest signal after photobleaching. Thus, 9793R and 9795R were the best suited polymers for this study. Of

the polymers tested, only 9795R and 9793R were subjected to the heat resiliency test. The 9793R did not delaminate after three minutes of heating, while the 9795R polymer showed warping. Thus 9793R was selected for further use.

Table 4- The results of auto-fluorescence experiments for each polymer.

Polymer name	Initial Fluorescence (V)	Experimental time(s)	Final Fluorescence (V)
9984	1.2	3500	0.6
9969	>5.5V	550	2
9964	>5.5V	2700	2
9962	1.2	2500	0.5
9960	>5.5V	550	4
9795R	0.36	1240	0.25
9793R	0.3	1886	0.2

The results of the circular well experiments are shown in **Figure 18**. The initial DNA solution (100 nM) had an RFU value of 2251. The Δ RFU values were determined by subtracting the fluorescence after agitating from this value; a higher Δ RFU indicates better capture. In this set of experiments, off chip sample vortexing had the best results with a Δ RFU 1200, 50 Hz had the lowest Δ RFU value of \sim 1000, and the control and 500 Hz were almost identical at \sim 1100. The standard *t*-test shows that there is no significant difference between vortexing and magnetic mixing, between the control and 500 Hz, or between 500 Hz and 50 Hz at the 95% confidence level. Thus, the circular geometry with these fields had no effect on mixing.

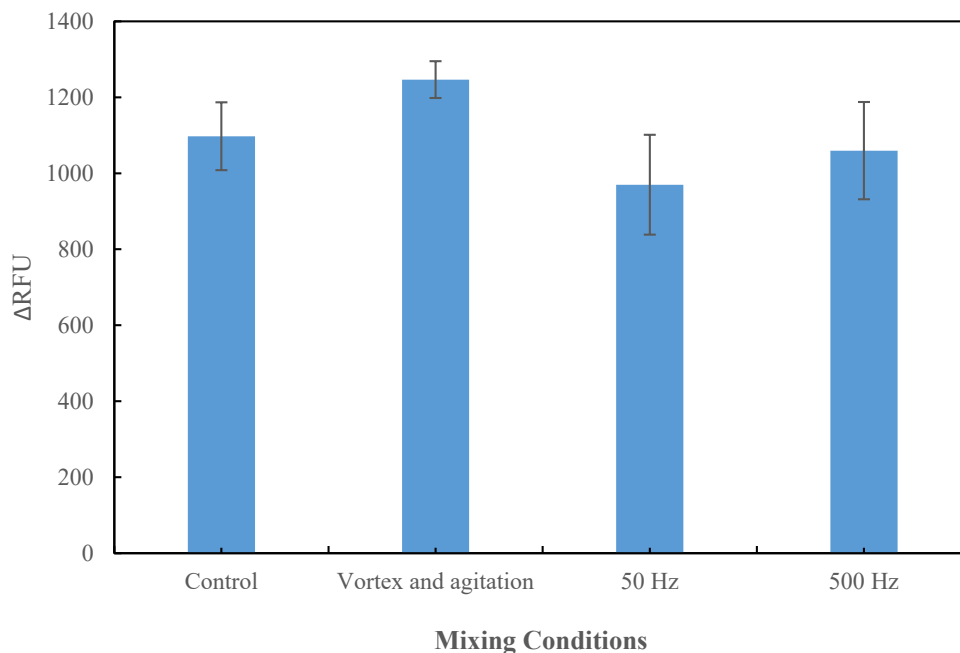


Figure 18- Δ RFU values for bead capture experiments in a circular well with flat cylindrical electromagnets.

The results for the diamond well experiments are shown in **Figure 19**. In this experiment the initial RFU for 100 nM DNA was 1491. The Δ RFU value increased from the control up to 100 Hz. The standard *t*-test indicates none of the experiments in **Figure 19** were statistically different at the 95% confidence level. Thus, the diamond shaped well with these fields had no effect on mixing.

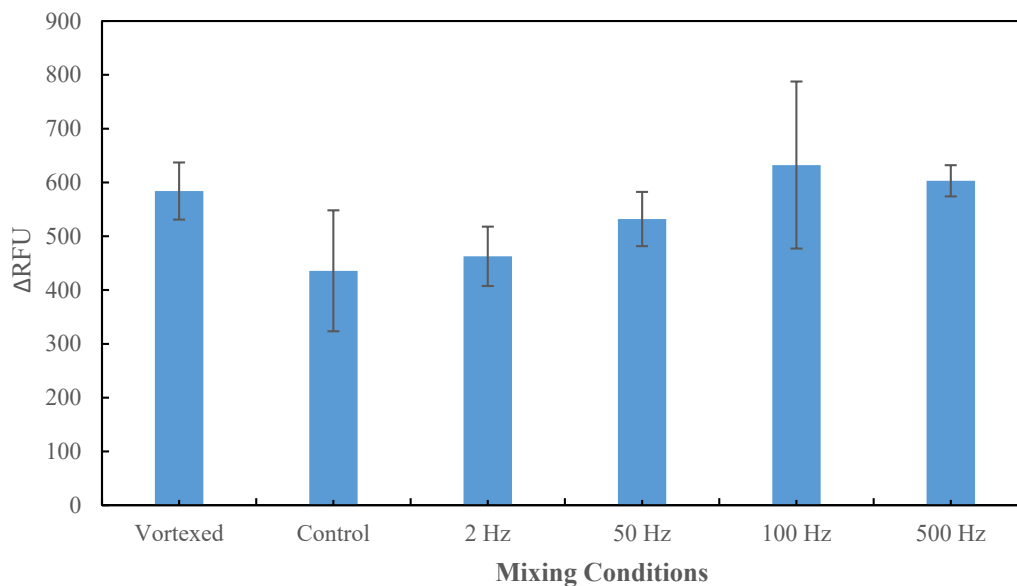


Figure 19- Results for signal generator experiments using the diamond well.

The results for the experiment using the DC power supply and a programmable Arduino chip are shown in **Figure 20**. The initial RFU value for 50 nM DNA was 511. The 100 Hz asymmetric condition had the largest Δ RFU value of 250, with a SD of 150. The *t*-test indicated that 100 Hz asymmetric was significantly different from the other methods at a 95% confidence interval. Vortexing and symmetric electromagnetic fields were not statistically different at the 95% confidence interval. All conditions, however, were significantly different from the control at the 95% confidence interval. However, this may be due to a problem with the control experiment, since with the same device geometry in **Figure 19**, there was no statistical difference between control and vortex experiments.

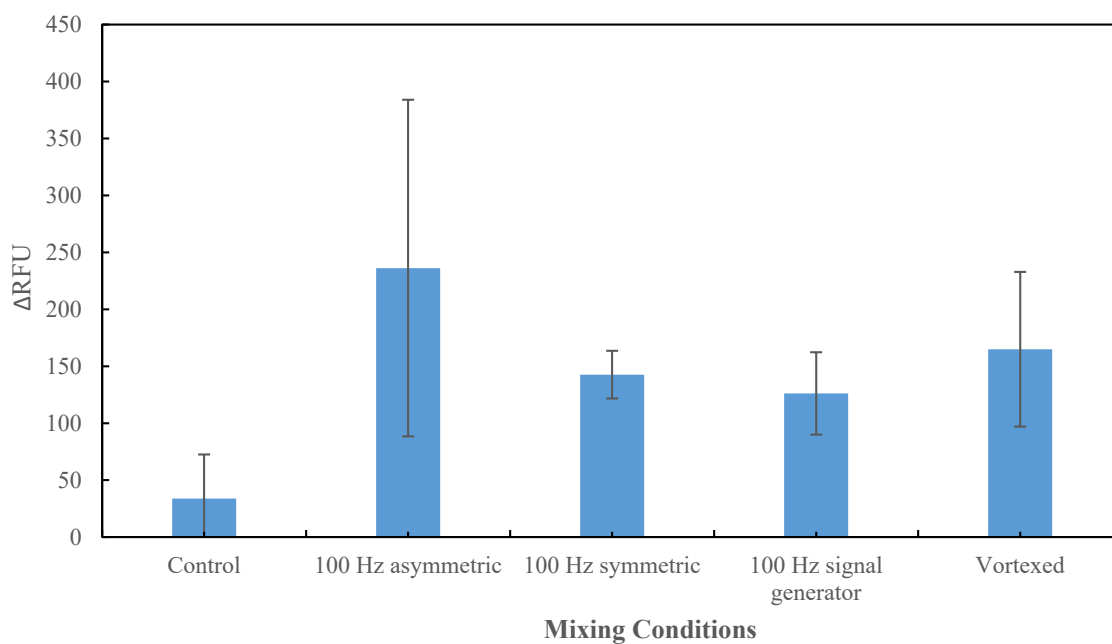


Figure 20-Results of the experiment using the Arduino Uno chip.

3.4- Conclusions

I demonstrated that micro wells and fluidic devices can be made with pressure sensitive adhesives. The only polymers with sufficiently low fluorescence were 9793R and 9795R; all other PSAs produced a high background signal even after photobleaching for more than an hour. Also, the other PSAs required a double-sided adhesive layer, because they did not have their own adhesive side; these extra layers compromised the structural integrity and increased probability of leaks.

I also demonstrated the use of an Arduino chip and MOSFET transistors instead of a signal generator to control voltage. The Arduino chip is significantly smaller and can fit on a microscope stand with the microfluidic chip. Tests showed that there was no significant difference between the symmetric Arduino chip mixing and the signal generator when they are both set to the same frequency. The Arduino system can be used for future mixing experiments.

Most of my experiments showed no significant difference between the control, where the beads are suspended in the DNA solution without any magnetic fields, and a condition where magnetic fields are in place. The main exception was asymmetric mixing. When the magnetic field rotated from one side of the well to another, capture efficiency improved. Future mixing wells should be designed with asymmetric magnetic fields in mind.

4. SUMMARY AND FUTURE WORK

4.1- Summary

This thesis reported different experiments involving laminar flow, PSA selection, and the fabrication of various mixing chambers. By doing the laminar flow experiments it was concluded that agitating and mixing the beads was necessary for optimal DNA capture. The PSA experiments demonstrated that only 9793R and 9795R were suitable for fluorescence detection experiments. The mixing chamber experiments had results that were comparable to vortex experiments which is an advantage, because this way efficient mixing can be done in an entirely closed system. However, it was observed that beads sitting in the chamber without any magnetic fields had similar capture efficiency to beads that were subjected to an electromagnetic field in many cases.

4.2-Future Work

To improve mixing and capture efficiency, different electromagnetic conditions should be tested. These conditions could include higher frequencies in the kHz or MHz range. Copper coils could also contain more coils to increase the magnetic field strength without increasing the current.

Besides magnetically induced agitation, different geometries have potential to improve mixing. For this reason, serpentine channels are commonly used ^[32]. A proposed design is to

have two intersecting serpentine channels as shown in **Figure 21**. This way beads and DNA can cross paths multiple times, increasing the probability of capture.

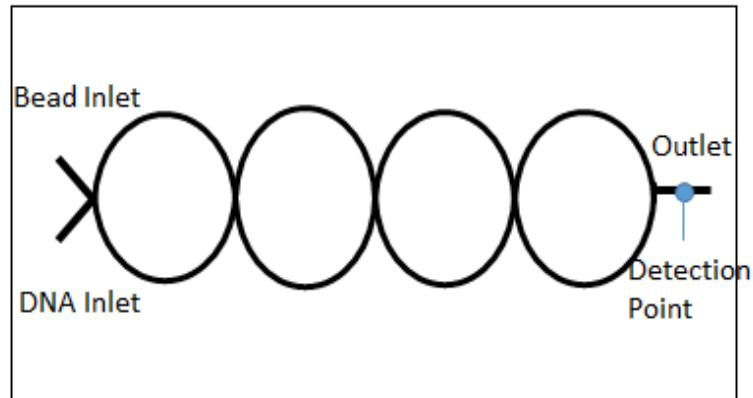


Figure 21- Design for a device with intersecting channels.

Flow through experiments with DNA and magnetic microbeads are a good way to test the capture efficiency of devices with intersecting channels. This can be done by fabricating the same chip design in in **Section 2.2**, but with PSAs and a laser cutter. To keep the beads in place, it may be necessary to create a monolith in the channel ^[49]. The monolith is a porous structure that will act like a filter, with DNA solution traveling through while beads remain trapped as shown in **Figure 22**. A laser on the other side of the monolith can be used to detect DNA.

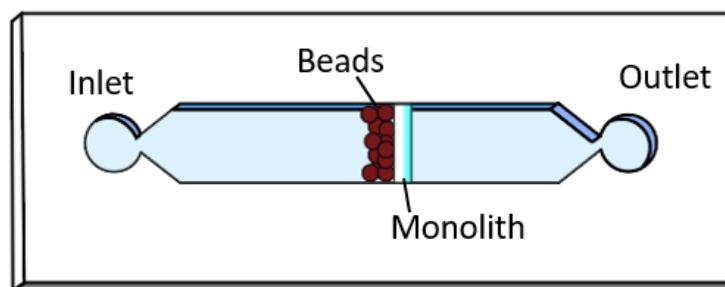


Figure 22- Device with porous monolith. Beads aggregate behind the monolith.

The ability to capture, enrich and detect specific DNA sequences at dilute concentrations can have a wide range of applications besides antibiotic resistant bacteria detection. Magnetic microbeads have already been used to extract and enrich trace DNA concentrations in poorly preserved ancient specimens, and cancer cells circulating in the bloodstream ^[23, 27]. Microfluidic based magnetic bead DNA capture also has the potential to isolate mRNA from cells to track development, as in the case of drug resistant cancer cells ^[55]. The ability to enrich picomolar DNA to detectable levels in a short amount of time will greatly enhance all of these abilities.

APPENDIX A-ARDUINO BASED AGITATION SYSTEM AND CODE

A.1- Wiring Diagram of EM Mixer

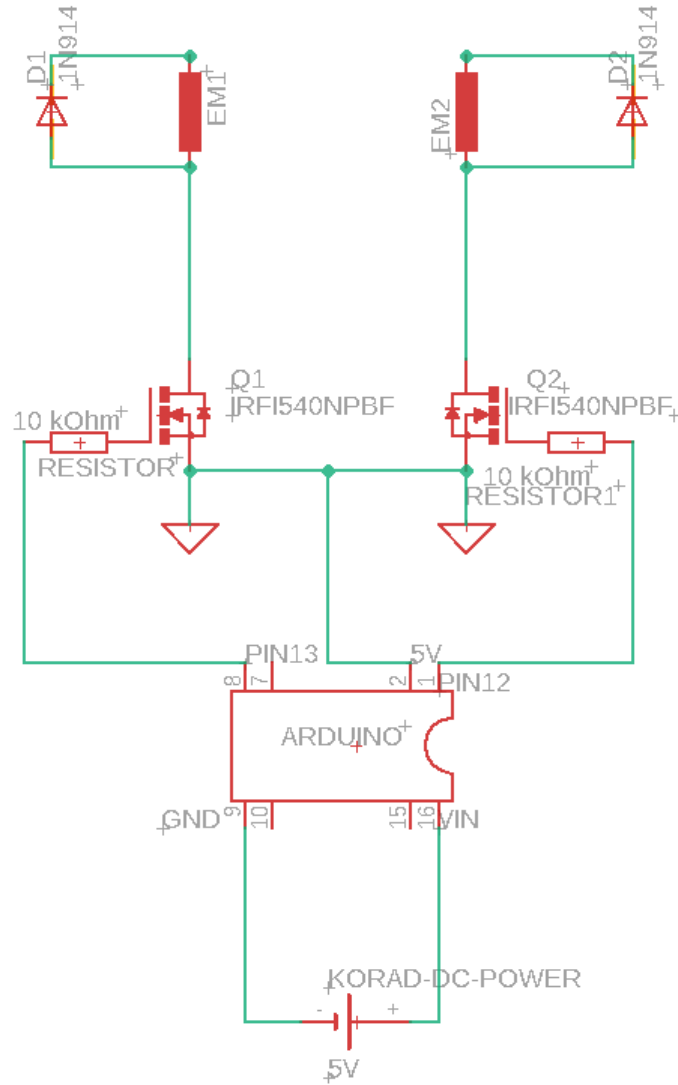


Figure A.1- A detailed wiring schematic of the electromagnetic micro mixer used in the DC based power experiments described in **Section 3.2**.

A.2- Code for Asymmetric Electromagnetic Mixer

```
sequentialblink_may21a | Arduino 1.8.9
File Edit Sketch Tools Help

sequentialblink_may21a

int EM1=13;
int EM2=12;

void setup() {
  // put your setup code here, to run once:
  pinMode(EM1,OUTPUT);
  pinMode(EM2,OUTPUT);
}
//this is so the other LED is completely off before the other one turnson
void loop() {
  // put your main code here, to run repeatedly:
  digitalWrite(EM1,HIGH); //turn on EM1
  delay(10); //wait for 10 ms
  digitalWrite(EM1,LOW); //turn off EM1
  //delay(10);
  digitalWrite(EM2,HIGH); //turn on EM2
  delay(10); //wait for 10 ms
  digitalWrite(EM2,LOW); //turn off EM2
  //delay(10); //wait for 10 ms
}
```

Figure A.2- Arduino code for the asymmetric mixer.

A.3- Code for Symmetric Electromagnetic Mixer



```
simultaneousblink_may21b | Arduino 1.8.9
File Edit Sketch Tools Help

simultaneousblink_may21b
int EM1=13;
int EM2=12;

void setup() {
  // put your setup code here, to run once:
  pinMode(EM1,OUTPUT);
  pinMode(EM2,OUTPUT);
}
//this is so the other LED is completely off before the other one turnson
void loop() {
  // put your main code here, to run repeatedly:
  digitalWrite(EM1,HIGH); //turn on EM1

  digitalWrite(EM2,HIGH); //turn on EM2
  delay(10);           //wait for 500 ms
  digitalWrite(EM2,LOW); //turn off EM2

  digitalWrite(EM1,LOW); //turn off EM1
  delay(10);
}
```

Figure A.3- Arduino code for symmetric mixer.

BIBLIOGRAPHY

1. Gul, F., et al., *Changing Definitions of Sepsis*. Turk J Anaesthesiol Reanim, 2017. **45**(3): p. 129-138.
2. Liu, V., et al., *Hospital deaths in patients with sepsis from 2 independent cohorts*. JAMA, 2014. **312**(1): p. 90-2.
3. Kreger, B.E., et al., *Gram-negative bacteremia. III. Reassessment of etiology, epidemiology and ecology in 612 patients*. The American Journal of Medicine, 1980. **68**(3): p. 12.
4. Yabupsky, P. and F.S. Nolte, *Quantitative Aspects of Septicemia*. Clinical Microbiology Review, 1990. **3**(3): p. 11.
5. Mayr, F.B., S. Yende, and D.C. Angus, *Epidemiology of severe sepsis*. Virulence, 2014. **5**(1): p. 4-11.
6. UK, N.H.S. *Antibiotics: Overview*. 2019 May 23, 2019 [cited 2019 July, 9]; Available from: <https://www.nhs.uk/conditions/antibiotics/>.
7. Zhou, Y., et al., *Detection of culture-negative sepsis in clinical blood samples using a microfluidic assay for combined CD64 and CD69 cell capture*. Anal Chim Acta, 2019. **1062**: p. 110-117.
8. Jesse T. Jacob, et al., *Vital Signs: Carbapenem-Resistant Enterobacteriaceae*, in *Morbidity and Mortality Weekly Report*. 2013, Center for Disease Control: MMWR website ((<http://www.cdc.gov/mmwr>)). p. 165-170.
9. Robledo, I.E., E.E. Aquino, and G.J. Vazquez, *Detection of the KPC gene in Escherichia coli, Klebsiella pneumoniae, Pseudomonas aeruginosa, and Acinetobacter baumannii during a PCR-based nosocomial surveillance study in Puerto Rico*. Antimicrob Agents Chemother, 2011. **55**(6): p. 2968-70.
10. Bratu, S., et al., *Carbapenemase-producing Klebsiella pneumoniae in Brooklyn, NY: molecular epidemiology and in vitro activity of polymyxin B and other agents*. J Antimicrob Chemother, 2005. **56**(1): p. 128-32.
11. Patel, G., et al., *Outcomes of carbapenem-resistant Klebsiella pneumoniae infection and the impact of antimicrobial and adjunctive therapies*. Infect Control Hosp Epidemiol, 2008. **29**(12): p. 1099-106.
12. Kumar, A., et al., *Duration of hypotension before initiation of effective antimicrobial therapy is the critical determinant of survival in human septic shock*. Crit Care Med, 2006. **34**(6): p. 1589-96.
13. Liu, C. and H.F. Chambers, *Staphylococcus aureus with Heterogeneous Resistance to Vancomycin: Epidemiology, Clinical Significance, and Critical Assessment of Diagnostic Methods*. Antimicrobial Agents and Chemotherapy, 2003. **47**(10): p. 3040-3045.
14. Shiota, S., et al., *Antibiotic Resistance of Helicobacter pylori Among Male United States Veterans*. Clin Gastroenterol Hepatol, 2015. **13**(9): p. 1616-24.
15. Cuny, C. and W. Witte, *PCR for the identification of methicillin-resistant Staphylococcus aureus (MRSA) strains using a single primer pair specific for SCCmec elements and the neighbouring chromosome-borne orfX*. Clin Microbiol Infect, 2005. **11**(10): p. 834-7.
16. Rocas, I.N. and J.F. Siqueira, Jr., *Detection of antibiotic resistance genes in samples from acute and chronic endodontic infections and after treatment*. Arch Oral Biol, 2013. **58**(9): p. 1123-8.

17. USFDA. *Film Array Blood Culture Identification Panel Kit*. 2013; Available from: http://www.accessdata.fda.gov/cdrh_docs/reviews/k130914.pdf.
18. Hedman, J. and P. Radstrom, *Overcoming inhibition in real-time diagnostic PCR*. *Methods Mol Biol*, 2013. **943**: p. 17-48.
19. Diekema, D.J. and M.A. Pfaller, *Rapid detection of antibiotic-resistant organism carriage for infection prevention*. *Clin Infect Dis*, 2013. **56**(11): p. 1614-20.
20. Wen, J., et al., *Microfluidic-Based DNA Purification in a Two-Stage, Dual-Phase Microchip Containing a Reversed-Phase and a Photopolymerized Monolith*. *Analytical Chemistry*, 2007. **79**(16): p. 8.
21. Baltekin, O., et al., *Antibiotic susceptibility testing in less than 30 min using direct single-cell imaging*. *Proc Natl Acad Sci U S A*, 2017. **114**(34): p. 9170-9175.
22. Pamme, N., *Magnetism and microfluidics*. *Lab Chip*, 2006. **6**(1): p. 24-38.
23. Emaus, M.N., M. Varona, and J.L. Anderson, *Sequence-specific preconcentration of a mutation prone KRAS fragment from plasma using ion-tagged oligonucleotides coupled to qPCR compatible magnetic ionic liquid solvents*. *Anal Chim Acta*, 2019. **1068**: p. 1-10.
24. Pereira-Barros, M.A., et al., *Direct PCR-free electrochemical biosensing of plant-food derived nucleic acids in genomic DNA extracts. Application to the determination of the key allergen Sola l 7 in tomato seeds*. *Biosens Bioelectron*, 2019. **137**: p. 171-177.
25. Feehery, G.R., et al., *A method for selectively enriching microbial DNA from contaminating vertebrate host DNA*. *PLoS One*, 2013. **8**(10): p. e76096.
26. Zhong, D. and W. He, *Detection of Pseudomonas aeruginosa in the Skin by Immunomagnetic Isolation and Real-Time Quantitative PCR*. *J Nanosci Nanotechnol*, 2019. **19**(9): p. 5517-5521.
27. Horn, S., *Target enrichment via DNA hybridization capture*. *Methods Mol Biol*, 2012. **840**: p. 177-88.
28. Mezger, A., et al., *A general method for rapid determination of antibiotic susceptibility and species in bacterial infections*. *J Clin Microbiol*, 2015. **53**(2): p. 425-32.
29. Khashan, S.A., A. Alazzam, and E.P. Furlani, *Computational analysis of enhanced magnetic bioseparation in microfluidic systems with flow-invasive magnetic elements*. *Sci Rep*, 2014. **4**: p. 5299.
30. Huang, G., et al., *A rapid, low-cost, and microfluidic chip-based system for parallel identification of multiple pathogens related to clinical pneumonia*. *Sci Rep*, 2017. **7**(1): p. 6441.
31. Croxatto, A., et al., *Laboratory automation in clinical bacteriology: what system to choose?* *Clin Microbiol Infect*, 2016. **22**(3): p. 217-35.
32. Nguyen, N.T. and S.T. Wereley, *Fundamentals and Applications of Microfluidics*. Second ed. 2006, Boston, USA: Norwood, MA.
33. Lee, C.Y., et al., *Microfluidic mixing: a review*. *Int J Mol Sci*, 2011. **12**(5): p. 3263-87.
34. Giuffrida, M.C. and G. Spoto, *Integration of isothermal amplification methods in microfluidic devices: Recent advances*. *Biosens Bioelectron*, 2017. **90**: p. 174-186.
35. Knob, R., et al., *Sequence-specific DNA solid-phase extraction in an on-chip monolith: Towards detection of antibiotic resistance genes*. *J Chromatogr A*, 2017. **1523**: p. 309-315.
36. Goh, C.S., et al., *Adhesive Bonding of Polymeric Microfluidic Devices*, in *11 th Electronics Packaging Technology Conference*. 2009: Singapore.

37. Popov, V.L., R. Pohrt, and Q. Li, *Strength of adhesive contacts: Influence of contact geometry and material gradients*. *Friction*, 2017. **5**(3): p. 308-325.
38. Wang, X., D. Nilsson, and P. Norberg, *Printable microfluidic systems using pressure sensitive adhesive material for biosensing devices*. *Biochim Biophys Acta*, 2013. **1830**(9): p. 4398-401.
39. A. Rida, T. Lehnert, and M.A.M. Gijs, *Microfluidic mixer using magnetic beads*, in *7th International Conference on Miniaturized Chemical and Biochemical Analytical Systems*. 2003: Squaw Valley, California.
40. Shikida, M., et al., *A palm-top-sized rotary-drive-type biochemical analysis system by magnetic bead handling*. *Journal of Micromechanics and Microengineering*, 2008. **18**(3).
41. Weddemann, A., et al., *Magnetic field induced assembly of highly ordered two-dimensional particle arrays*. *Langmuir*, 2010. **26**(24): p. 19225-9.
42. Lee, S.H., et al., *Effective mixing in a microfluidic chip using magnetic particles*. *Lab Chip*, 2009. **9**(3): p. 479-82.
43. Buchanan, C.M., et al., *Rapid separation of very low concentrations of bacteria from blood*. *J Microbiol Methods*, 2017. **139**: p. 48-53.
44. Wood, R.L., et al., *An experimental investigation of interfacial instability in separated blood*. *AIChE Journal*, 2019. **65**(4): p. 1376-1386.
45. Hawkins, A.R. and H. Schmidt, *Optofluidic waveguides: II. Fabrication and structures*. *Microfluid Nanofluidics*, 2007. **4**(1-2): p. 17-32.
46. Schmidt, H. and A. Hawkins, *Optofluidics waveguides: I. Concepts and implementations*. *Microfluidics and Nanofluidics*, 2008. **4**(1-2): p. 14.
47. Ozcelik, D., et al., *Optofluidic wavelength division multiplexing for single-virus detection*. *Proc Natl Acad Sci U S A*, 2015. **112**(42): p. 12933-7.
48. Alizadeh, M., et al., *Rapid separation of bacteria from blood - Chemical aspects*. *Colloids Surf B Biointerfaces*, 2017. **154**: p. 365-372.
49. Knob, R., et al., *Sequence-specific sepsis-related DNA capture and fluorescent labeling in monoliths prepared by single-step photopolymerization in microfluidic devices*. *J Chromatogr A*, 2018. **1562**: p. 12-18.
50. Kim, J.Y. and D. O'Hare, *Monolithic nano-porous polymer in microfluidic channels for lab-chip liquid chromatography*. *Nano Converge*, 2018. **5**(1): p. 19.
51. Cai, H., et al., *Optofluidic analysis system for amplification-free, direct detection of Ebola infection*. *Sci Rep*, 2015. **5**: p. 14494.
52. Lukacs, G.L., et al., *Size-dependent DNA mobility in Cytoplasm and Nucleus*. *Journal of Biological Chemistry*, 2000. **275**(3): p. 5.
53. Bird, B.R., W.E. Stewart, and E.N. Lightfoot, *Transport Phenomena*. Second Edition ed. 2006: John Wiley & Sons, Inc.
54. Atkins, P.W., *Physical Chemistry*, . 5 ed. 1994, New York: W.H. Freeman.
55. Shao, H., et al., *Chip-based analysis of exosomal mRNA mediating drug resistance in glioblastoma*. *Nat Commun*, 2015. **6**: p. 6999.